ELECTRICAL ENGINEERING AND ENERGY

OPEN ACCESS

Reliability-Oriented Design and Sizing of a Standalone Solar PV-Battery Chick Brooding System under the Cool Highland Climate of Mbeya, Tanzania

Emily Yohana Mwalyagile[1], Owdean Suwi[1], and Joel Mbwiga[2]

[1] Department of Electrical and Power Engineering, College of Engineering and Technology, Mbeya University of Science and Technology, Mbeya, Tanzania
[2] Department of Mechanical and Industrial Engineering, College of Engineering and Technology, Mbeya University of Science and Technology, Mbeya, Tanzania

Submitted: 19 October 2026
Accepted : 31 October 2026
Online First:6 November 2026

Corresponding author,
Emily Yohana Mwalyagile
mwalyagilecan@gmail.com

DOI:
10.64470/elene.2026.45

RESEARCH ARTICLE

Copyright, Authors, Distributed under Creative Commons CC-BY 4.0

Abstract: Though the heating need often matches poor or very variable energy access, reliable chick brooding in cold mountain regions calls for constant heat during the first weeks after hatching. For a standalone solar photovoltaic (PV)-battery brooder serving 80 chicks under the climatic conditions of Mbeya, Tanzania, this study created a reliability-oriented design and simulation framework. An age-dependent thermal-load model was matched with a cleaned 2023–2025 dataset comprising 1,096 aligned daily records of maximum temperature, minimum temperature, and sunshine duration. For Week 1, the mean modeled electrical heating demand was 3.73 kWh/day, while the 95th-percentile demand was 5.20 kWh/day. January sunshine of 3.11 h/day and a PV performance ratio of 0.75 yielded a theoretical PV requirement of 2.23 kWp utilizing the conservative design load; the ultimate array was raised to 2.60 kWp. Three-day battery sizing with 24 V, 80% maximum depth of discharge and 90% battery efficiency resulted in 902.78 Ah, hence guiding choice of a 1000 Ah bank. Both PV supply and heating demand were reconstructed hourly and the battery was dispatched chronologically over thirty-six 28-day cycles. Final design reached a mean loss of load probability (LLP) of 0.1087%, a maximum cycle LLP of 3.9130%, a minimum state of charge (SOC) of 20.0% and a mean heating-energy compliance of 99.8913%. Only the January 2024 cycle had 1.589 kWh of significant unmet heating energy. The model thus suggests great technical dependability under the given assumptions; prototype validation is still needed before purchases or field deployment.

Keywords Solar photovoltaic, Battery storage, Chick brooding, Days of autonomy, State of charge, Loss of load probability.

1. Introduction

In poultry production, the first few weeks after hatching are a brief but demanding stage. Because their ability to regulate body temperature is limited until they reach adulthood, newborn chicks require warm environments (Henriksen et al., 2016). As a result, recommended brooding temperatures are maximum during the first week and gradually decrease as the birds get older. Recent research on broilers also shows that stress response and thermal preference change rapidly during the early stages of development (Wijnen

et al., 2022). Heat loss during this period may have a detrimental effect on survival, growth, and well-being; as a result, brooding is no longer a postponable load but rather a dependability-critical energy service.

In the cool highland climate of Mbeya, there can be a significant difference between the surrounding temperature and the desired setpoint, particularly at night and during the chilly period from June to August. Recent research conducted in Tanzania indicates that small-scale chicken farming encounters significant challenges related to production and management, such as housing, diseases, feed, and flock supervision issues (Ngongolo & Chota, 2021; Wilson et al., 2022). High chick mortality rates can lead to considerable financial setbacks for small-scale farmers (Ngongolo & Chota, 2022). Solar-electric brooding is attractive because heat can be regulated automatically, but the design problem remains demanding because the thermal load continues through the night while solar generation is intermittent.

Standalone photovoltaic (PV) systems are becoming more and more popular for off-grid rural uses since they are modular and can be installed close to the place of consumption (Baurzhan & Jenkins, 2016). Greater focus is also being placed on decentralized renewable energy solutions in African food, water, and energy applications (Mperejekumana et al., 2024). But yearly or monthly energy balance by itself is inadequate for a welfare-critical thermal demand. While an undersized battery can lose heating service overnight, an undersized array might not recover storage following low-solar days. Conversely, too much oversizing increases capital expense without always providing commensurate dependability.

In standalone PV design, this trade-off is often understood. Together with careful consideration of load variation, resource availability, autonomy, depth of discharge, conversion losses, and dependability (Khatib et al., 2016), array and storage capacities should be chosen. Particularly helpful are state-of-charge (SOC) and loss-of-load indicators as they reveal whether energy is accessible when needed, not just if long-term production surpasses long-term demand (Quiles et al., 2020). For poultry, renewable heating technologies hold technical promise, particularly when thermal management and enclosure performance are taken in concert (Cui et al., 2020). Solar incubation and automated poultry systems both highlight the need of combining renewable supply with sensing and control (Kyeremeh & Peprah, 2017; Peprah et al., 2022).

A remaining engineering gap is the lack of a locally parameterized workflow that combines age-dependent brooding demand, seasonal climate variability in Mbeya, conservative PV sizing, explicit three-day battery autonomy, chronological state-of-charge tracking, and quantitative reliability indicators. This study therefore aims to: (i) estimate electrical heating demand across the four brooding weeks; (ii) size the PV array and battery bank using the conservative Week-1 demand and three-day nominal autonomy; (iii) evaluate reliability over 36 independent, monthly-start, 28-day simulation cycles from 2023 to 2025 using SOC, loss of load probability (LLP) and heating-energy compliance and (iv) assess the sensitivity of reliability to PV and battery capacities. The principal contribution is a reliability-oriented sizing framework that distinguishes the low-sunshine storage-recovery challenge in January from the high heating-load challenge in July.

2. System Configuration and Methodology

2.1. Study area, climatic data and data-quality control

The study covered Mbeya District in Tanzania's Southern Highlands. Approximately 8°57'42" S, 33°21'24" E is the representative district reference point. The model utilized 1,096 aligned daily records of maximum temperature, minimum temperature, and sunshine duration spanning January 2023 to December 2025. By date, the three climate series were combined and checked for missing values, non-negative sunshine duration, and the physical need Tmax ≥ Tmin. Four erroneous numbers found during the audit were fixed utilizing source string interpretation, next-day continuity, and physical stability. This quality-control phase was kept in the research record to allow replication of the ultimate dependability results and temperature data. The geographical location used to represent the study area is shown in Figure 1.

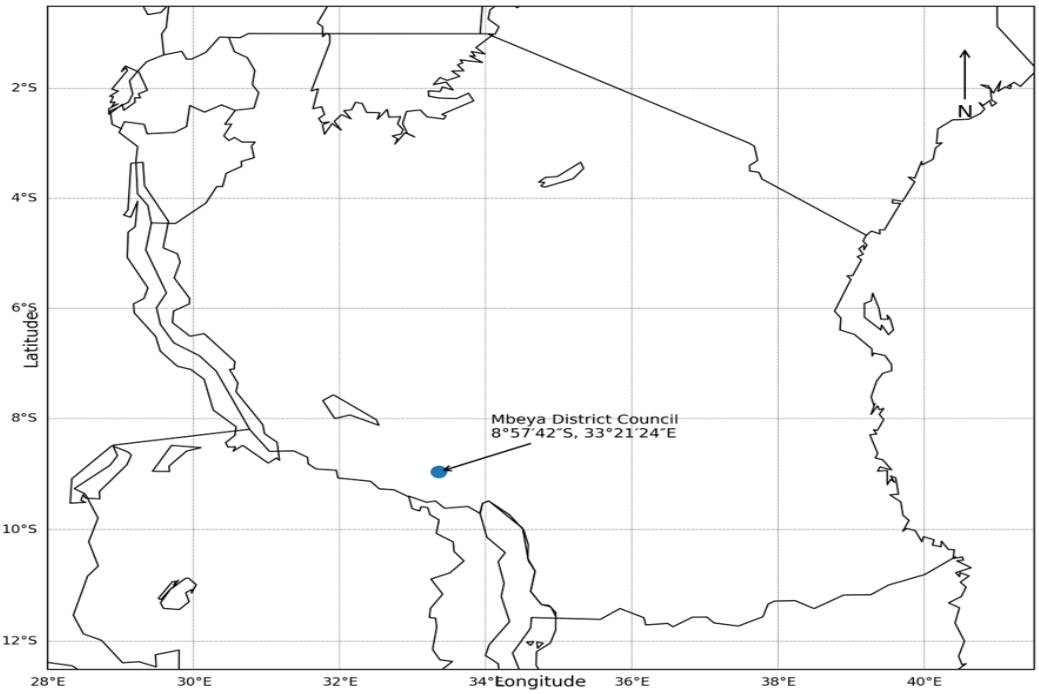


Figure 1. Location of the Mbeya District study area in Tanzania, showing the representative GPS reference point used for geographical presentation.

Instead of being handled as measured hourly data, hourly ambient temperature was reconstructed from the daily extrema. In the simplified PV-energy model, sunshine duration served as an efficient solar-resource proxy. In addition to defining constraints that should be examined during prototype field validation, these presumptions allow climate-driven design analysis from the available Tanzania Meteorological Authority (TMA) observations.

2.2. Physical system architecture and brooder thermal model

The proposed standalone brooding system comprises a photovoltaic array, a maximum power point tracking (MPPT) charge controller, a 24 V battery bank, a protected direct current (DC) bus, a thermostat-controlled resistive heater and a chick-level temperature sensor. The insulated 2 m × 3 m × 2 m enclosure houses 80 chicks. The building heat-balance method follows standard agricultural enclosure calculations (L. P. Bengtsson, 1986) . Assuming heat transfer through the six faces, the effective area is 32 m², and the study-specific assumed overall heat-transfer coefficient is U = 0.45 W m-2 K-1.

The brooding phase consists of four seven-day stages, with target temperatures set at 34.0, 31.5, 29.0, and 26.5 °C for weeks one through four, respectively. Estimated sensible metabolic heat production for each stage is 1.0, 1.4, 1.8, and 2.2 W per chick. The heating system is modeled as a 24 V DC resistive load, assuming an energy-delivery efficiency (η_h) of 0.95. While the incremental decrease in temperature follows standard poultry brooding practices, these specific setpoints are chosen for this scenario rather than serving as universal husbandry requirements. Operational temperatures should be adjusted based on chick behavior, breed, humidity levels, housing environment, and sensor placement.

The adopted U-value, chick sensible-heat inputs, heater efficiency, PV performance ratio (PR = 0.75), maximum depth of discharge (DoD = 0.80) and battery energy-delivery efficiency (ηbat = 0.90) are engineering assumptions rather than experimentally validated values. Age-related brooding-temperature requirements and chick responses are discussed in poultry research (Henriksen et al., 2016; Wijnen et al., 2022) . The PVWatts manual (Dobos, 2014) addresses PV modeling losses; it does not validate the brooder thermal inputs, or the selected PR. Component datasheets and measured data would be needed for field validation.

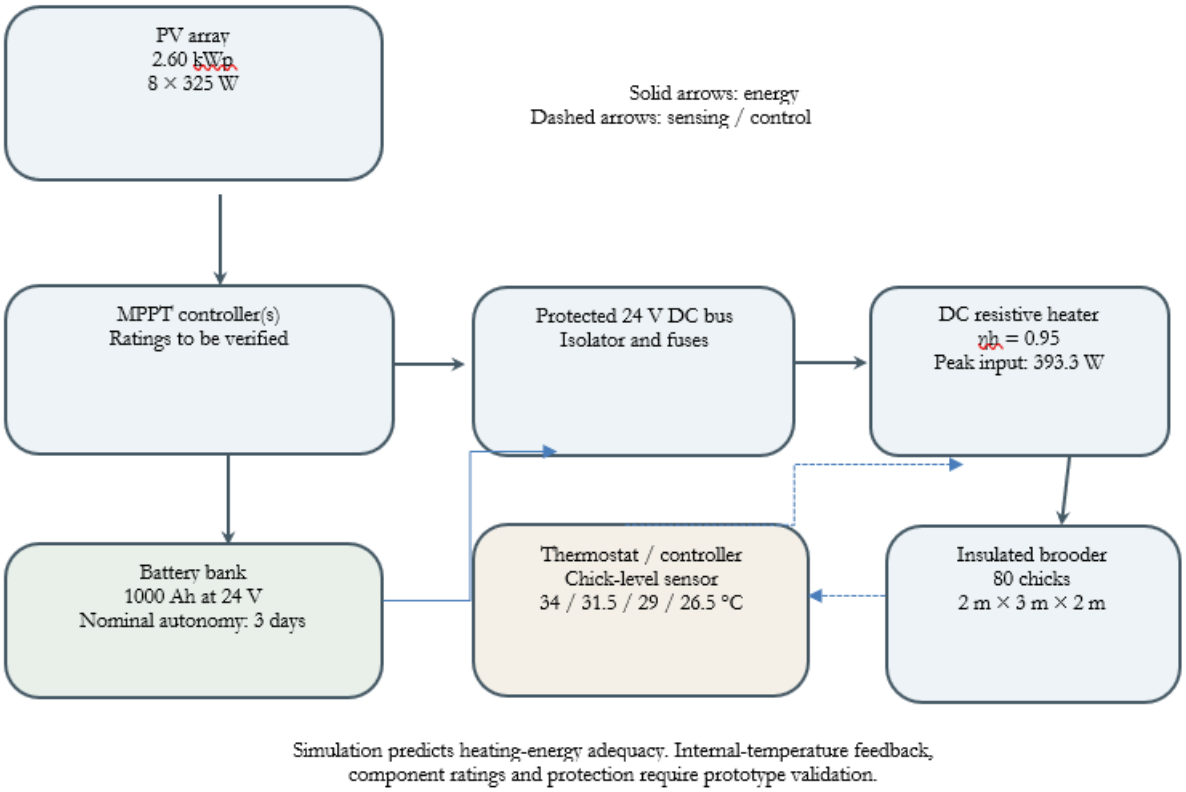


Figure 2. Proposed PV–battery brooder architecture and energy/control flow for the 2.60 kWp array and 1000 Ah battery at 24 V.

Hourly conductive heat loss through the enclosure was calculated as:

$$Q_{\text{loss},t} = UA\max\left(T_{\text{set},t} - T_{\text{amb},t},\ 0\right) \tag{1}$$

Chick metabolic heat and the resulting net external heating requirement were calculated from:

$$Q_{\text{met},t} = Nq_{\text{chick},t} \tag{2}$$

$$Q_{\text{net},t} = \max\left(Q_{\text{loss},t} - Q_{\text{met},t},\ 0\right) \tag{3}$$

The electrical heater input was then:

$$P_{\text{heater},t} = \frac{Q_{\text{net},t}}{\eta_h} \tag{4}$$

The resulting weekly electrical-load characteristics are summarized in Table 1.

Table 1. Brooding electrical-load characteristics used in system design

Week	Setpoint (°C)	Mean demand (kWh/day)	95th percentile (kWh/day)	Peak electrical power (W)	Heating-active fraction (%)
1	34.0	3.73	5.20	393.3	99.6
2	31.5	2.10	3.48	321.7	85.1
3	29.0	0.92	2.02	250.1	53.2
4	26.5	0.26	1.00	178.5	22.2

For Table 2, the mean, standard deviation (SD), 95th-percentile daily electrical-heating demand and nominal 95 percent confidence interval (CI) of the mean were computed as mean ± 1.96 SD/√1,096 for each brooding week from the 1,096 modeled daily climate records. The percentile uses linear interpolation at rank

1 + 0.95(n − 1), where n = 1,096. Descriptive variability statistics were employed in place of hypothesis tests between treatment groups because this is a deterministic engineering simulation rather than a randomized biological experiment. The variability statistics for the modeled daily heating demand are summarized in Table 2.

Table 2. Variability of modeled daily electrical-heating demand across the 1,096 climate days

Week	Mean (kWh/day)	SD (kWh/day)	Nominal 95% CI of mean	P95 (kWh/day)
1	3.73	0.82	3.68–3.78	5.20
2	2.10	0.74	2.06–2.14	3.48
3	0.92	0.56	0.89–0.95	2.02
4	0.26	0.35	0.24–0.28	1.00

2.3. Hourly temperature reconstruction and load aggregation

The daily temperature extrema were converted to an hourly profile using a sinusoidal approximation:

$$T_{\text{amb},d,h} = T_{\text{mean},d} + T_{\text{amp},d}\cos\left[\frac{\pi(h-15)}{12}\right] \quad (5)$$

where $T_{mean} = \frac{(Tmax + Tmin)}{2}$ and $T_{amp} = \frac{(T_{max} - T_{min})}{2}$. The sinusoidal approximation places the modeled daily maximum at about 15:00 and the minimum at about 03:00; these are assumptions, not measured hourly observations. The hourly heater energy is summed to obtain the daily electrical demand and its Week-1 upper-tail distribution.

2.4. PV array and three-day battery sizing

Rather than from the four-week mean, the PV array was sized from the demand of the 95th percentile during Week-1. With only 3.11 hours per day, January had the least amount of sunshine over the month. Given a PV performance ratio of 0.75, the cautious analytical PV capacity was:

$$\text{PPV} = \frac{E_{design}}{PSH \times PR} = \frac{5.20}{3.11 \times 0.75} = 2.23 \text{ kWp} \quad (6)$$

Seven 325 W modules (2.275 kWp) have comparable analytical value. To offer more generating reserve, the last simulated array was raised to 2.60 kWp, matching eight 325 W panels.

For three days of nominal autonomy, battery storage was precisely sized. The final equation takes into account both acceptable depth of discharge and battery efficiency, in contrast to a simplified Ah calculation:

$$C_{bat} = \frac{E_{design} \times N_{aut} \times 1000}{V_{sys} \times DoD \times \eta_{bat}} \quad (7)$$

$$C_{bat} = \frac{5.20 \times 3 \times 1000}{24 \times 0.80 \times 0.90} = 902.78 \text{ Ah} \quad (8)$$

The selected bank had 1000 Ah at 24 V, rounded up. With a nominal energy of 24.0 kWh, it can provide 17.28 kWh of usable storage after 80% DoD and 90% battery efficiency. Before accounting for concurrent PV recharge, this corresponds to roughly 3.32 days at the 5.20 kWh/day design load.

2.5. Sensitivity analysis and chronological hourly simulation

The nine combinations of PV and battery capacities represent a sensitivity analysis rather than a formal mathematical or economic optimization. Three photovoltaic capacities (2.08, 2.60, and 3.12 kWp) were assessed alongside three battery capacities (700, 1000, and 1300 Ah). The 2.60 kWp/1000 Ah setup was chosen as a reliability-focused engineering design within the examined range; no assertion of a universally optimal cost or capacity is presented. Figure 3 encapsulates climate data processing, hourly load and PV reconstruction, sequential dispatch, and reliability evaluation. Every one of the 36 individual monthly-start

cycles includes 672 hourly segments and begins at 100% battery state of charge (SOC). The integrated simulation workflow is presented in Figure 3.

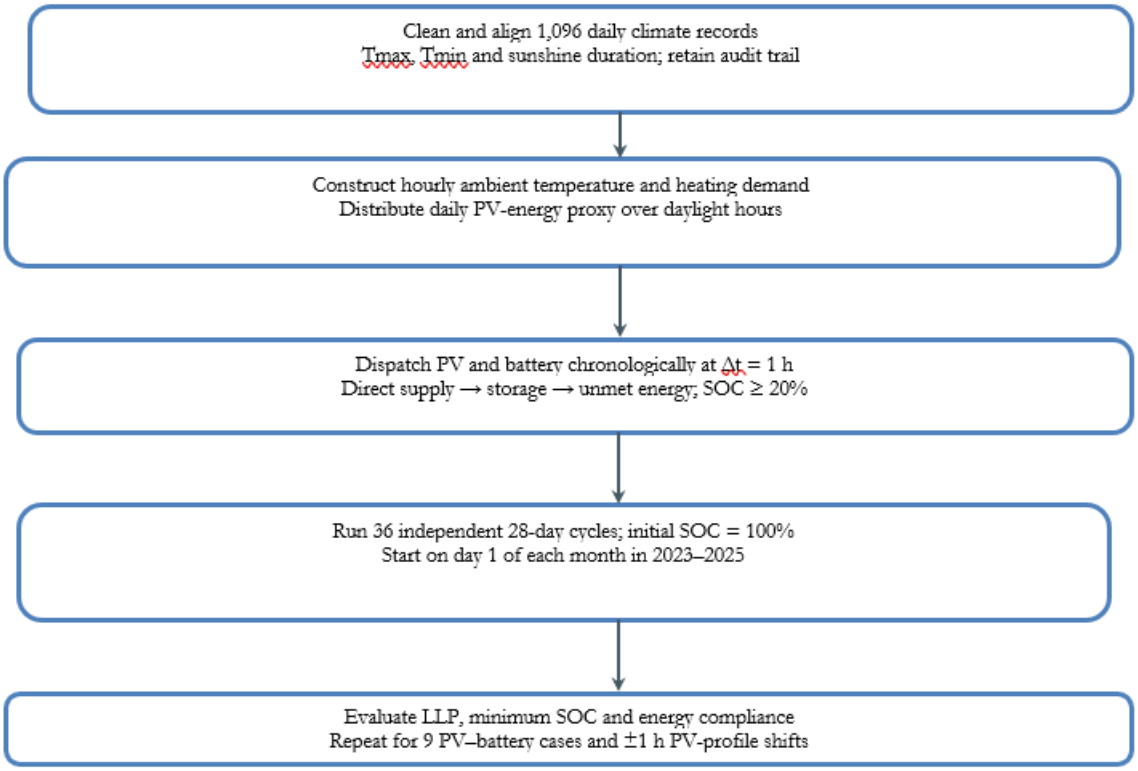


Figure 3. Workflow for climate processing, reconstructed hourly temperature and PV supply, hourly thermal demand, chronological battery dispatch and sensitivity analysis.

The chronological reliability computation uses a one-hour time step (Δt = 1 h) for both reconstructed PV supply and heater demand. Each of the 36 independent monthly-start brooding cycles comprises 672 consecutive hourly intervals and begins with a fully charged battery (SOC = 100%). PV generation first serves the concurrent heating demand; only the remaining energy charges the battery, and stored energy supports deficits subject to the SOC floor. Generation in a later hour cannot compensate for an earlier unmet load. The same dispatch rules are applied to all nine PV–battery combinations.

For each one-hour interval t, required heater electrical energy (kWh) is computed from electrical power (W) and the dispatch interval (h):

$$E_{load,t} = \frac{P_{heater,t}\,\Delta t}{1000} \tag{9}$$

To retain the defined daily sunshine-duration energy proxy while imposing hourly daylight generation, hourly PV energy is allocated as follows:

$$E_{PV,d,h} = P_{PV}\,PR\,s_d\,w_h \tag{10}$$

$$w_h = \frac{\cos[\pi(h-6)/12] - \cos[\pi(h-5)/12]}{2}, 6 \le h \le 17 \tag{11}$$

Here, s_d is the observed daily sunshine duration (h/day), not irradiance-derived peak-sun hours. Outside the assumed 06:00–18:00 daylight window, wh = 0; within that window the twelve hourly weights sum to one. Equation (11) integrates a normalized half-sine over each one-hour interval and therefore conserves the estimated daily PV energy exactly. For clarity, the daily PV-energy proxy is $E_{PV,d} = P_{PV} \times PR \times sd$, and hourly energy is $E_{PV,d,h} = EPV,d \times wh$. The assumed profile does not describe measured cloud timing, sunrise or sunset.

The retained PR of 0.75 represents losses occurring before the battery in this proxy model. Battery losses are treated separately so that double counting is avoided. DoD = 0.80 and η_{bat} = 0.90 are retained assumptions rather than values certified for a particular battery. One lumped loss factor is assigned to discharge, while charging is treated as ideal, giving a modeled charge–discharge round-trip efficiency of 90%. This allocation is a bookkeeping device for the simplified model; it does not assert that a real battery charges without losses, since actual efficiency depends on operating condition.

$$B_{nom} = \frac{V_{sys}\, C_{bat}}{1000};\ B_{min} = (1 - DoD)\, B_{nom}; \tag{12}$$

B_t is nominal stored energy in kWh at the start of interval t. For PV surplus, $E_{PV,t} \geq E_{load,t}$, storage is updated by:

$$B_{t+1} = \min(B_{nom}, B_t + E_{PV,t} - E_{load,t}) \tag{13}$$

For a deficit, $E_{PV,t} < E_{load,t}$, the stored energy and unmet heating energy are:

$$B_{t+1} = \max(B_{min}, B_t - \frac{E_{load,t} - E_{PV,t}}{\eta_{bat}}) \tag{14}$$

$$E_{unmet,t} = \max(E_{load,t} - E_{PV,t} - \eta_{bat}(B_t - B_{min}), 0) \tag{15}$$

In intervals with a surplus, unmet energy equals zero. Any surplus that storage cannot absorb is curtailed. SOC is computed following each storage update; this energy-only model neither borrows future PV energy nor applies any limit on charge/discharge power:

$$SOC_{t+1} = 100\frac{B_{t+1}}{B_{nom}} \tag{16}$$

A timing sensitivity check moves the entire daily PV profile forward by one hour and back by one hour, while keeping the daily energy intact. This assesses how sensitive results are to the assumed profile timing; it does not serve to validate the unknown observed hourly irradiance.

3. Reliability Evaluation Framework

3.1. Performance indicators

LLP is the percentage of needed electrical heating energy over a 28-day cycle that could not be delivered:

$$\text{LLP} = \frac{\sum E_{unmet}}{\sum E_{load}} \times 100 \tag{17}$$

Battery state of charge (SOC) is monitored on an hourly basis, with a 20% minimum SOC limit reflecting an 80% maximum depth of discharge. Heating-energy compliance is measured as the percentage of modeled heating energy provided; these energy metrics do not serve as direct indicators of specific chick-level temperature or welfare outcomes.

$$\text{Compliance} = 100(1 - \frac{E_{unmet}}{E_{load}}) = 100 - \text{LLP} \tag{18}$$

3.2. Sensitivity cases and model boundary

Sensitivity analysis looked at PV capacity values of 2.08, 2.60, and 3.12 kWp against battery capacity levels of 700, 1000, and 1300 Ah. The 700 Ah and 1300 Ah cases are sensitivity perturbations around the adopted 1000 Ah three-day design; they are not alternative claims that every tested battery size provides three days of autonomy. Outside the approved energy model were battery aging, rate-capacity effects, complex temperature dependency, cable losses, controller clipping, and dynamic internal brooder thermal mass.

4. Results and Discussion

4.1. Climate-resource and brooding-load interaction

Figure 4 illustrates the seasonal distribution of sunshine duration, estimated PV energy availability, and modeled brooding-heating demand. Sunshine duration peaked in August (9.18 h/day) and reached its lowest monthly mean in January (3.11 h/day). Although July recorded the highest Week-1 heating demand (4.99 kWh/day), it also benefited from relatively high sunshine duration (8.66 h/day). Consequently, the month with the highest heating requirement did not necessarily present the greatest risk for battery recovery.

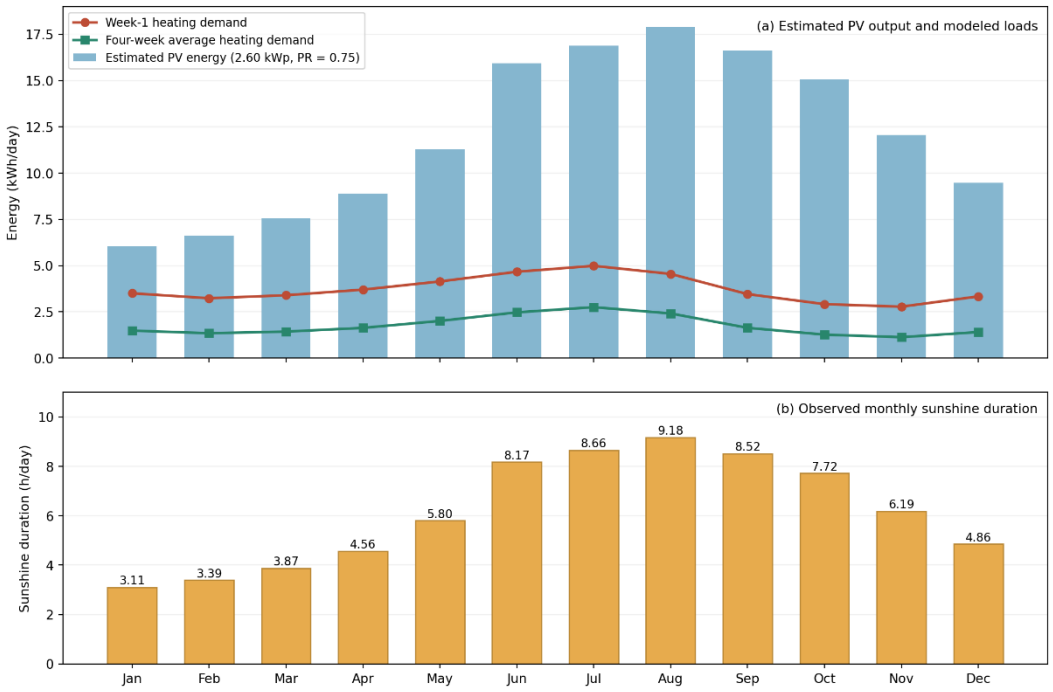


Figure 4. Monthly distribution of observed sunshine duration and comparison of estimated PV energy potential for the 2.60 kWp array with modeled Week-1 and four-week average brooding-heating demand in Mbeya, 2023–2025. PV energy is a sunshine-duration-based estimate, not measured generation.

The January stretch with little sunshine restricts the recovery of storage, even though its heating demand stays below the July peak. As a result, chronological dispatch reveals information that comparisons of monthly or cycle-total energy are unable to capture. The solar-energy values shown in Figure 4 are still dependent on the sunshine-duration proxy.

4.2. Final PV and battery sizing

Sizing from the average four-week demand of roughly 1.75 kWh/day under average sunlight would have resulted in a PV need of only roughly 0.38 kWp. That value serves as a lower-bound energy estimate, but it is useless for a welfare-sensitive thermal load. The theoretical PV requirement was raised to 2.23 kWp using the January solar resource and Week-1 95th-percentile demand. Thus, the chosen 2.60 kWp array provides a purposeful margin of generation.

The three-day battery equation produced 902.78 Ah at 24 V when 80% DoD and 90% battery efficiency were taken into account. Selecting 1000 Ah provides about 10.8 percent capacity leeway in relation to the estimated Ah demand and helps prevent rounding below the projected need. The usable delivered storage exceeds the three-day design energy of 15.6 kWh by 1.68 kWh at 17.28 kWh. The final PV and battery sizing results are summarized in Table 3.

Table 3. PV and battery sizing results

Sizing item	Value	Engineering interpretation
Average four-week load	1.75 kWh/day	Lower-bound energy indicator
Week-1 95th-percentile load	5.20 kWh/day	Conservative design load
Minimum monthly sunshine	3.11 h/day	Critical PV-resource input
Theoretical PV requirement	2.23 kWp	Conservative analytical size
Final PV array	2.60 kWp	Eight 325 W modules; generation reserve
Required battery capacity	902.78 Ah @ 24 V	Three-day design with DoD and ηbat
Selected battery bank	1000 Ah @ 24 V	Practical rounded capacity
Usable delivered storage	17.28 kWh	After 80% DoD and 90% efficiency

4.3. Reliability of the final three-day configuration

During the 36 monthly-start cycles, the final 2.60 kWp/1000 Ah configuration fulfilled nearly all of the projected brooding-heating requirements. The mean LLP was 0.1087%; the maximum LLP observed was 3.9130%; the minimum SOC recorded was 20.0%; the average compliance for heating energy was 99.8913%; and the minimum compliance stood at 96.0870%, as illustrated in Table 4. These results support the assessment of the final design as highly reliable under the simulated conditions, although it cannot be classified as a completely zero-deficit system.

Table 4. Reliability indicators for the final 2.60 kWp PV/1000 Ah system

Indicator	Hourly simulation result
Mean LLP	0.1087%
Maximum cycle LLP	3.9130%
Minimum SOC	20.00%
Mean heating-energy compliance proxy	99.8913%
Minimum heating-energy compliance proxy	96.0870%

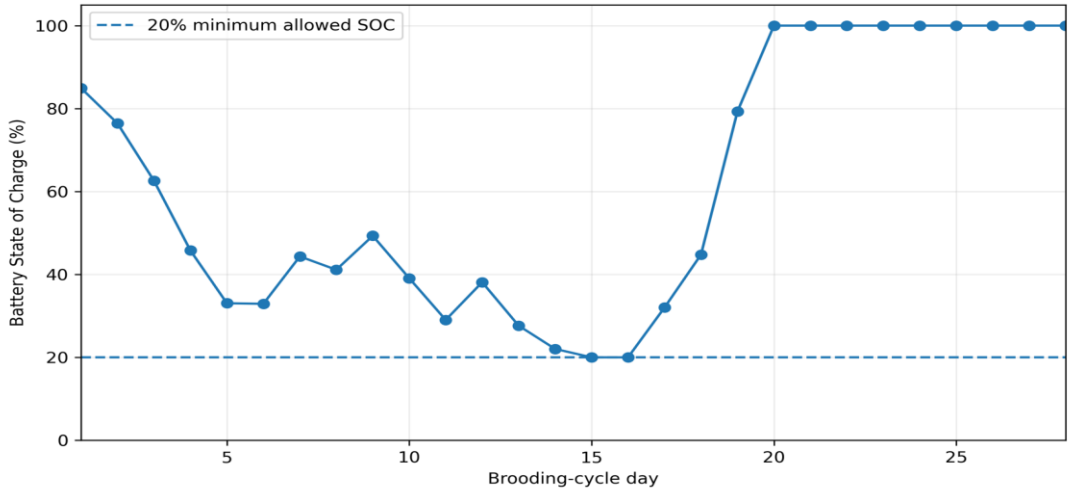


Figure 5. Battery SOC during the worst 28-day brooding cycle beginning 1 January 2024. The 20% line is the minimum allowable operating SOC.

Figure 6 presents cycle LLP and minimum hourly SOC for every monthly start in 2023–2025.

The most adverse cycle begins on 1 January 2024 (Figure 5). Its modeled heating demand is 40.612 kWh, while its PV-energy proxy totals 66.495 kWh; however, 1.589 kWh remains unmet over 33 hourly intervals. The battery falls to the 20% SOC floor before subsequent PV production enables it to recover. A daily aggregate comparison case applied to the same climate inputs yields 0.474 kWh of unmet energy and a worst-cycle LLP of 1.1677%, compared with 3.9130% under chronological hourly dispatch. Mean LLP is 0.0324%

in the daily aggregate case and 0.1087% in the hourly case. The comparison shows how daily aggregation can conceal intra-day shortfalls.

Shifting the assumed daylight PV profile forward by one hour produces a mean LLP of 0.1007% and a maximum cycle LLP of 3.6237%; shifting it back by one hour produces 0.1152% and 4.1478%, respectively. The same January 2024 starting point continues to be the worst cycle. These limited timing changes support the chronology finding but do not substitute for measured hourly irradiance or quantify the complete uncertainty in the sunshine-to-energy conversion.

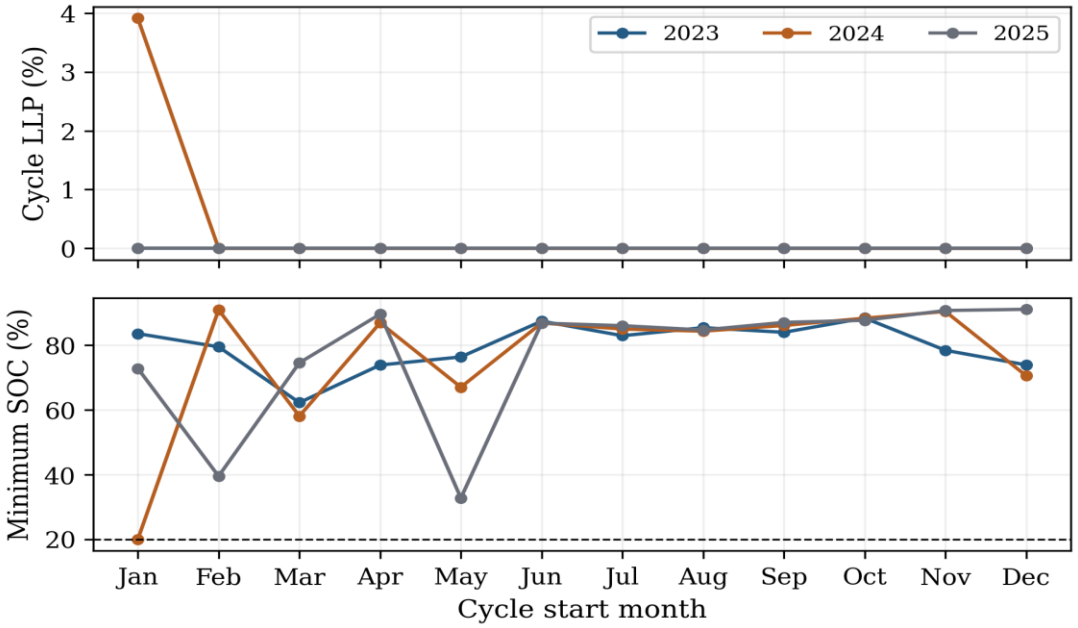


Figure 6. Monthly-start cycle LLP and minimum hourly SOC for the 2.60 kWp/1000 Ah configuration in 2023–2025.

4.4. PV-battery sensitivity and interpretation of the design envelope

The complete nine-case PV–battery sensitivity results are summarized in Table 5. The PV-battery sensitivity relationship is presented in Figure 7. The sensitivity analysis shows that modeled energy reliability generally improves when PV generation or battery capacity is increased. At 2.60 kWp, increasing storage from 700 to 1000 Ah reduces mean LLP from 0.6616% to 0.1087%, while 1300 Ah yields no unmet heating energy in the tested cycles. At 1000 Ah, increasing PV capacity from 2.08 to 2.60 and 3.12 kWp reduces mean LLP from 0.3711% to 0.1087% and 0.0000%, respectively. The 2.08 kWp/1300 Ah case has mean LLP of 0.0165%. Zero modeled shortfall is conditional on the proxy climate reconstruction, model assumptions and independent full-SOC starts; comparing additional capacity requires a specified reliability target and lifecycle-cost evidence.

Table 5. PV–battery sensitivity results from hourly chronological dispatch over 36 independent cycles

PV (kWp)	Battery (Ah)	Mean cycle LLP (%)	Maximum cycle LLP (%)	Minimum SOC (%)
2.08	700	1.0379	26.1249	20.00
2.08	1000	0.3711	13.3602	20.00
2.08	1300	0.0165	0.5954	20.00
2.60	700	0.6616	16.6778	20.00
2.60	1000	0.1087	3.9130	20.00
2.60	1300	0.0000	0.0000	32.80
3.12	700	0.3200	8.1962	20.00
3.12	1000	0.0000	0.0000	28.59
3.12	1300	0.0000	0.0000	45.07

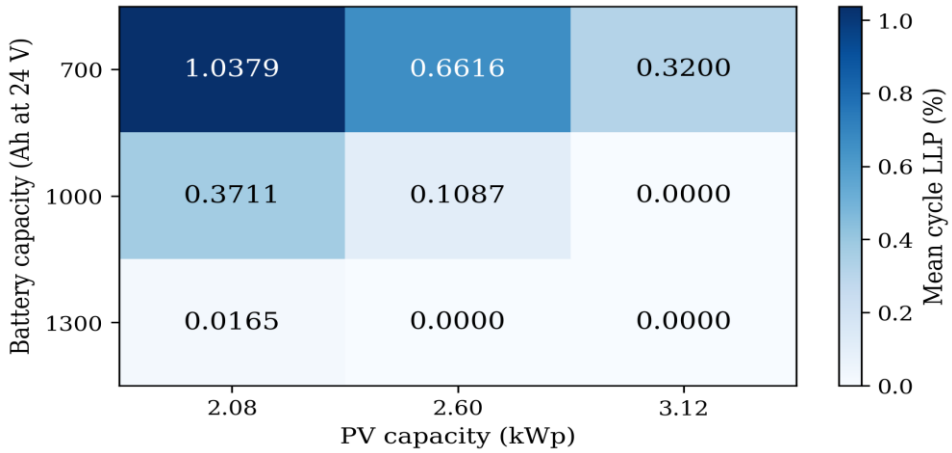


Figure 7. Sensitivity of average LLP to PV capacity and battery capacity.

4.5. Electrical hardware checks and storage-recovery considerations

At a 24 V DC bus, a 2.60 kW PV input equates to about 108.3 A before converter losses, thermal derating, and manufacturer-recommended safety margins are taken into account. This serves as a sizing reference at the nominal bus voltage rather than a prediction of the operating current at every moment. At that voltage, an 80 A battery-side charger would restrict transfer from the full array. The final MPPT configuration must be verified against the module open-circuit voltage (Voc), voltage at maximum power (Vmp), short-circuit current (Isc), string arrangement, controller input-voltage limits, and rated output current. Depending on the selected component datasheets, a higher-current controller or compatible controllers connected in parallel may be necessary.

The heater circuit needs its own current and protection assessment. Week-1 peak modeled electrical input is 393.3 W, corresponding to approximately 16.4 A at 24 V. Protection selection must consider conductor ampacity, continuous-load duty, thermostat contact ratings, short-circuit protection and permissible voltage drop. Battery isolation, PV disconnection, appropriate DC fuses or breakers, low-voltage cutoff and over-temperature protection require verification against the final hardware specification.

Nominal battery autonomy and post-deficit recharge time are separate design criteria. The calculated PV requirement of 2.23 kWp was derived from a conservative heating load of 5.20 kWh/day and the mean January sunshine duration, with the chosen 2.60 kWp array offering an additional generation margin. Nevertheless, analytical sizing does not ensure that a battery depleted during extended periods of low sunlight can be fully restored within a set timeframe while still powering the brooder. If rapid recovery is necessary, a recovery-time constraint must be assessed through chronological dispatch, accounting for concurrent heating demands, PV generation, and battery charging limits. Additionally, the independent 28-day cycles assume a full state of charge (SOC) and do not account for continuous operation across consecutive months.

4.6. Practical implementation, protection and field-validation pathway

To enhance the efficiency of small-scale brooding, it is essential to prioritize enhancing dependability by focusing on thermal regulation and suitable monitoring instead of solely relying on the inclusion of PV modules. Enhancing insulation and sealing air leaks can decrease energy consumption directly, and adjusting temperature settings as chicks grow older can prevent unnecessary heating. A practical setup for on-site testing should include temperature sensors at chick level, a programmable thermostat for control, monitoring of heater status and energy usage, alarms for low battery and temperature levels, and the possibility of remote monitoring through GSM/IoT technology. Recent advanced poultry energy systems exhibit similar characteristics (Okonkwo et al., 2025; Peprah et al., 2022). It is important to confirm the final MPPT design and the current rating of the controller by referring to the actual component datasheets before purchasing.

Field validation needs to monitor various factors such as outdoor air temperature, brooder temperature inside at chick level, plane-of-array irradiance or PV power, heater power, and battery state of charge (SOC) at a brief enough logging frequency to record thermostat operations and instances of low solar power. It is recommended to conduct tests during at least one cold-weather cycle and one cycle with low sunlight in January or February. Following this, the accuracy of the model should be evaluated by calculating the mean absolute error (MAE) and root-mean-square error (RMSE) for temperature and energy, as well as by comparing the predicted and actual SOC trajectories.

4.7. Limitations and contribution

The research is still a design exercise based on simulations. Hourly temperatures are derived from daily maximum and minimum values, while hourly PV supply is produced using a daily sunshine-duration proxy and an assumed daylight profile. There are no measured hourly irradiance or PV-output datasets to validate either the magnitude or the timing within each day. Sunshine duration does not account for diffuse irradiation under overcast conditions and cannot determine plane-of-array energy yield. Using a fixed daylight period also fails to reflect seasonal changes in sunrise and sunset times. The U-value, chick sensible-heat inputs, heater efficiency, PV derating, DoD, and battery efficiency are scenario inputs that have not been validated. The thermal model does not include ventilation heat loss, infiltration dynamics, thermal mass, or spatial temperature differences. Battery aging, electrochemical and rate-capacity effects, temperature dependence, and hardware power limitations are likewise omitted. Heating-energy compliance evaluates delivered energy rather than chick temperature or welfare. Starting each cycle with a fully charged independent system does not demonstrate uninterrupted operation across multiple cycles.

Within these limitations, the contribution integrates an age-dependent thermal load with local daily climate observations, conservative first-week sizing, explicit three-day autonomy, and hourly SOC/LLP assessment. July produces the maximum modeled thermal demand, whereas January presents the greatest challenge for storage recovery in the tested cycles. This distinction can inform prototype sizing and field-test selection, but establishing absolute reliability requires calibrated irradiance, component, and thermal measurements.

5. Conclusions

A standalone PV–battery chick-brooding system was designed and modeled for 80 chicks in a 12 m^3 enclosure under the cool highland climate of Mbeya. Week 1 required an average electrical heating demand of 3.73 kWh/day and a 95th-percentile daily demand of 5.20 kWh/day (not a peak hourly demand); Week 4 averaged approximately 0.26 kWh/day. The modeled peak electrical heater input during Week 1 was 393.3 W. Conservative sizing gave a 2.23 kWp PV requirement and 902.78 Ah of nominal battery capacity for three days of autonomy with an 80% maximum DoD and 90% battery energy-delivery efficiency. The selected reference configuration uses eight 325 W modules (2.60 kWp) and a 1000 Ah battery at 24 V.

The modeled reference configuration achieved mean LLP of 0.1087%, maximum cycle LLP of 3.9130%, minimum SOC of 20.0% and mean heating-energy compliance of 99.8913%. Only the January 2024-start cycle recorded unmet electrical heating energy: 1.589 kWh of the 40.612 kWh demand. The hourly result is more conservative than the daily aggregate comparison because it preserves the timing of supply and demand. Among the nine capacity cases, 3.12 kWp/1000 Ah and 2.60 kWp/1300 Ah both achieved zero modeled shortfalls under the assumed profile. These are sensitivity findings, not evidence of a global optimum or field-validated reliability.

Prior to being deployed in the field, it is advised to create an advanced prototype that includes precise temperature detection for chicks, measuring irradiance and PV power, monitoring heater power, logging battery state of charge (SOC), and recording thermostat and control status. The data collected should be utilized to confirm the accuracy of the thermal model, battery energy balance, and protective control needs, before finalizing the design as a procurement specification.

Nomenclature

A	Effective brooder heat-transfer area (m^2)
C_{bat}	Battery-bank capacity (Ah)
DoD	Maximum allowable depth of discharge (fraction)
E_{design}	Rounded daily electrical design load (kWh/day)
LLP	Loss of load probability, defined here as unmet heating-energy percentage (%)
N	Number of chicks
PR	Performance ratio used here as an assumed PV-to-DC-bus derating factor excluding battery losses (fraction)
s_{design}	January mean observed sunshine duration used for conservative PV sizing (h/day); not peak-sun hours
SOC_t	Battery state of charge at hourly boundary t (%)
U	Overall enclosure heat-transfer coefficient (W m^{-2} K^{-1})
η_{bat}	Lumped battery energy-delivery efficiency, allocated to discharge (fraction)
η_h	Heater energy-delivery efficiency (dimensionless)
Compliance	Cycle heating energy delivered as a percentage of required heating energy; 100% − LLP (%)
Π	Circle constant used in the sinusoidal reconstruction (dimensionless)
B_t	Nominal energy stored at hourly boundary t (kWh)
B_{nom}	Nominal maximum stored battery energy (kWh), consistently used in Equations (12), (13), and (16)
B_{min}	Stored-energy floor imposed by DoD (kWh)
$E_{load,t}$	Electrical heating energy required in interval t (kWh)
E_{load}	Total required electrical heating energy over a cycle (kWh)
$E_{PV,d,h}$; $E_{PV,t}$	Reconstructed PV energy in day d and clock-hour h, or elapsed interval t (kWh)
$E_{unmet,t}$	Unmet heating energy in hourly interval t (kWh)
E_{unmet}	Total unmet heating energy over a cycle (kWh)
E_{usable}	Usable delivered battery energy after DoD and the lumped loss factor (kWh)
P_{PV}	Installed PV nameplate capacity (kWp)
$P_{heater,t}$	Electrical heater input power at interval t (W)
$Q_{loss,t}$	Enclosure conductive heat-loss rate at interval t (W)
$Q_{met,t}$	Total chick sensible-heat production at interval t (W)
$Q_{net,t}$	Net external thermal-heating rate at interval t (W)
$q_{chick,t}$	Assumed sensible-heat production per chick for the applicable age group (W per chick)
$T_{set,t}$	Brooding temperature setpoint applicable to hourly interval t (°C)
$T_{amb,t}$; $T_{amb,d,h}$	Reconstructed ambient temperature at elapsed interval t or day d and clock-hour h (°C)
T_{max}; T_{min}; $T_{max,d}$; $T_{min,d}$	Observed maximum and minimum temperatures, with d identifying the calendar day (°C)
$T_{mean,d}$	Mean of the daily maximum and minimum temperatures (°C)
$T_{amp,d}$	Half the daily maximum–minimum temperature difference (K)
V_{sys}	Nominal DC bus voltage (V)
N_{aut}	Nominal battery autonomy (days)
s_d; s_{design}	Daily measured sunshine duration and rounded January mean used for preliminary sizing (h/day)
w_h	Normalized fraction of daily PV energy assigned to clock-hour h (dimensionless); zero outside the assumed 06:00–18:00 daylight window, with Σh wh = 1
t; d; h	Elapsed hourly interval index; calendar-day index; clock-hour index (h = 0, …, 23)
Δt	Length of one chronological simulation interval (h); Δt = 1 h in this study
N	Number of daily climate observations used for descriptive load statistics (n = 1,096; dimensionless)
V_{oc}; V_{mp}	PV module open-circuit voltage and voltage at maximum power (V)
I_{sc}	PV module short-circuits current (A)
PV	Photovoltaic
MPPT	Maximum power point tracking
DC	Direct current
TMA	Tanzania Meteorological Authority
SD; CI	Standard deviation; confidence interval
MAE; RMSE	Mean absolute error; root-mean-square error
GSM; IoT	Global System for Mobile Communications; Internet of Things
kWp; Ah	Kilowatt peak (PV nameplate rating); ampere-hour
η_h	Legacy heater-efficiency symbol, standardized to η_h throughout the model
SOC_{t+1}	Battery state of charge at the end of interval t (start of interval t + 1), expressed as a percentage of Bnom
∑h	Summation over the clock-hour intervals h of a day; Σh wh = 1 (dimensionless)

Declaration of Ethical Standards

As the authors of this study, we declare that we comply with all ethical standards.

Simulation was done based on published data on brooding parameters along with engineering/climatic data. No animal experiment or human-based experiment was performed; hence, there was no need to seek any approval for the simulation work.

Credit Authorship Contribution Statement

• E. Y. Mwalyagile: Conceptualization, Methodology, Software, Formal analysis, Visualization, Writing – original draft.

• O. Suwi : Supervision, Methodology, Writing -review and editing.

• J. Mbwiga: Supervision, Methodology, Writing - review and editing.

Declaration of Competing Interest

The authors declared that they have no conflict of interest.

Acknowledgements

The authors acknowledge the institutional environment that supported this research.

Funding

The authors did not receive specific external funding for this research.

Data Availability

The daily climate data were obtained from the Tanzania Meteorological Authority (TMA). They comprise the maximum and minimum temperatures and sunshine duration for 2023–2025; the hourly profiles are model-reconstructed inputs rather than measured hourly observations. Processed inputs, the text-cleaning audit and the hourly calculation results are available from the authors subject to applicable data-use terms.

References

Baurzhan, S., & Jenkins, G. P. (2016). Off-grid solar PV: Is it an affordable or appropriate solution for rural electrification in Sub-Saharan African countries? *Renewable and Sustainable Energy Reviews*, *60*, 1405–1418. https://doi.org/10.1016/j.rser.2016.03.016

Bengtsson, L. P., & Whitaker, J. H. (Eds.). (1986). *Farm structures in tropical climates: A textbook for structural engineering and design*. FAO. https://openknowledge.fao.org/handle/20.500.14283/s1250e

Cui, Y., Theo, E., Gurler, T., Su, Y., & Riffat, S. (2020). A comprehensive review on renewable and sustainable heating systems for poultry farming. International Journal of Low-Carbon Technologies, 15(1), 121–142. https://doi.org/10.1093/ijlct/ctz048

Dobos, A. P. (2014). *PVWatts version 5 manual* (Technical Report NREL/TP-6A20-62641). National Renewable Energy Laboratory. https://www.nrel.gov/docs/fy14osti/62641.pdf

Henriksen, S., Bilde, T., & Riber, A. B. (2016). Effects of post-hatch brooding temperature on broiler behavior, welfare, and growth. *Poultry Science*, *95*(10), 2235–2243. https://doi.org/10.3382/ps/pew224

Khatib, T., Ibrahim, I. A., & Mohamed, A. (2016). A review on sizing methodologies of photovoltaic array and storage battery in a standalone photovoltaic system. *Energy Conversion and Management*, *120*, 430–448. https://doi.org/10.1016/j.enconman.2016.05.011

Kyeremeh, F., & Peprah, F. (2017). Design and construction of an Arduino microcontroller-based egg incubator. *International Journal of Computer Applications*, *168*(1), 15–23. https://doi.org/10.5120/ijca2017914261

Mperejekumana, P., Shen, L., Gaballah, M. S., & Zhong, S. (2024). Exploring the potential and challenges of energy transition and household cooking sustainability in sub-sahara Africa. *Renewable and Sustainable Energy Reviews*, *199*, 114534. https://doi.org/10.1016/j.rser.2024.114534

Ngongolo, K., & Chota, A. (2021). Chicken production, flock size, management systems, and challenges in the Dodoma region in Tanzania. *Poultry Science*, *100*(6), 101136. https://doi.org/10.1016/j.psj.2021.101136

Ngongolo, K., & Chota, A. (2022). Effect of sex, age, diseases, and control intervention on chickens' mortality and its financial implications in Dodoma, Tanzania. *Poultry Science*, *101*(5), 101785. https://doi.org/10.1016/j.psj.2022.101785

Okonkwo, W. I., Ejiogu, E., Ojike, O., Ezenne, G. I., Idika, I. K., & Onyechi, A. U. (2025). Solar-powered Trombe wall brooding of day-old poultry chicks. *International Journal of Poultry Science*, *24*(1), 31–36. https://doi.org/10.3923/ijps.2025.31.36

Peprah, F., Gyamfi, S., Amo-Boateng, M., Buadi, E., & Obeng, M. (2022). Design and construction of smart solar powered egg incubator based on GSM/IoT. *Scientific African*, *17*, e01326. https://doi.org/10.1016/j.sciaf.2022.e01326

Quiles, E., Roldán-Blay, C., Escrivá-Escrivá, G., & Roldán-Porta, C. (2020). Accurate sizing of residential stand-alone photovoltaic systems considering system reliability. *Sustainability*, *12*(3), 1274. https://doi.org/10.3390/su12031274

Wijnen, H. J., Molenaar, R., Kemp, B., van Roovert-Reijrink, I. A. M., van den Brand, H., & van der Pol, C. W. (2022). Effects of late incubation temperature and moment of first post-hatch feed access on neonatal broiler development, temperature preference, and stress response. *Poultry Science*, *101*(10), 102088. https://doi.org/10.1016/j.psj.2022.102088

Wilson, W. C., Slingerland, M., Oosting, S., Baijukya, F. P., Smits, A. J., & Giller, K. E. (2022). The diversity of smallholder chicken farming in the Southern Highlands of Tanzania reveals a range of underlying production constraints. *Poultry Science*, *101*(10), 102062. https://doi.org/10.1016/j.psj.2022.102062